Theoretical study of small aluminum phosphide and magnesium sulfide clusters

Mohammad A. AlLaham, Gary W. Trucks, and Krishnan Raghavachari

Citation: The Journal of Chemical Physics **96**, 1137 (1992); doi: 10.1063/1.462201
View online: http://dx.doi.org/10.1063/1.462201
View Table of Contents: http://scitation.aip.org/content/aip/journal/jcp/96/2?ver=pdfcov
Published by the AIP Publishing

Theoretical study of small aluminum phosphide and magnesium sulfide clusters

Mohammad A. Al-Laham, Gary W. Trucks,[a] and Krishnan Raghavachari
AT&T Bell Laboratories, Murray Hill, New Jersey 07974

(Received 22 July 1991; accepted 3 October 1991)

Electronic structures and stabilities of small Al_nP_n and Mg_nS_n clusters ($n = 1$–3) are explored by means of accurate quantum chemical calculations. The effects of polarization functions and electron correlation are included in these calculations. Ionic factors are clearly dominant for MgS clusters. Thus, both Mg_2S_2 and Mg_3S_3 have planar ground state geometries where charge alternation is utilized effectively. AlP clusters, on the other hand, behave intermediate between the ionic MgS clusters and the covalent Si clusters. Thus, while the ground state structures of Al_2P_2 and Al_3P_3 are both analogous to those of the isoelectronic silicon clusters Si_4 and Si_6, other low-lying minima which are similar to those of MgS clusters are also present. The hybridization and bonding in the different structures are discussed.

INTRODUCTION

The structures and properties of small clusters have been the subject of numerous investigations by means of a variety of experimental and theoretical studies in recent years.[1-29] Most of these studies have focused on clusters formed from a single element and have yielded many novel and unexpected results.[1-20] In particular, group IV clusters such as carbon[1-4] and silicon,[5-12] and alkali metal clusters such as sodium[13] or potassium[14] have received a lot of attention. Covalently bonded nonmetallic clusters such as phosphorus[16,17] and sulfur[18-20] have also been studied, but to a lesser extent.

In contrast to elemental clusters, much less work has been carried out in the case of mixed clusters containing more than one element. Among these, maximum attention has been focused on III–V clusters such as GaAs[21-25] due to their obvious technological importance. Recent spectroscopic work has been performed on InP to yield information on electronic excited states of small clusters.[26] Novel condensed phase clusters have been observed for other semiconductor systems such as ZnS or CdSe.[27]

Ab initio calculations on elemental clusters (such as carbon or silicon) have been invaluable in providing geometries and electronic structures and have led to a better understanding of their physical properties and chemical reactivities.[4,12] However, theoretical studies on mixed clusters have been limited due to the computational difficulties associated with such systems.[24,25,28,29] In addition to the larger number of geometrical structures which have to be considered, mixed clusters have the complications associated with permutational variations resulting from the presence of several elements. The nature of the bonding can also show a larger variation ranging from ionic to covalent to metallic bonding.

In this work, we report our results from detailed *ab initio* molecular orbital calculations on the structures and energies of III–V and II–VI mixed clusters. In particular, we have studied the monomers, dimers, and trimers of AlP and MgS. Our motivations in this study are severalfold. First, the clusters considered are isoelectronic with the silicon clusters Si_2, Si_4, and Si_6. These are systems on which we have previously performed detailed theoretical studies to understand their structures and properties.[5,11,12] Thus, it is of interest to consider the changes introduced by the inclusion of heteroatoms in these clusters. Second, we want to consider the structures of the clusters as the bonding becomes more ionic as we go from Si to AlP to MgS. Our study shows clearly that clusters of AlP behave intermediate between Si clusters and MgS clusters. For example, Al_3P_3 exhibits different minima which are analogous to Si_6 (covalent) and Mg_3S_3 (ionic) structures. The hybridization and bonding in these structures will be discussed in detail. Finally, the structures of AlP clusters are being used as starting points to perform detailed investigations of III–V clusters containing heavier elements (e.g., GaAs).[29]

THEORETICAL METHODS

The geometrical parameters for several different starting structural and electronic (singlet, triplet, etc.) arrangements were optimized completely using gradient techniques at the Hartree–Fock (HF) level of theory.[30] Initial optimizations were performed using the Slater-type orbital (STO)-3G[31] and the 3-21G*[32] basis sets. For the promising structures, the final optimization was performed using the 6-31G*[33] (valence double-zeta *sp* plus a set of *d* type polarization functions on each atom) basis set. Though this basis set is not of double-zeta quality in the core region, it is known to produce reliable results for isoelectronic silicon clusters.[12] For each structure, the complete set of harmonic force constants and the associated vibrational frequencies were then evaluated using analytical second derivative techniques at the HF/6-31G* level.[34] The vibrational frequencies were used to determine if a given calculated structure is a local minimum. Zero-point energies were calculated at the HF/6-31G* level and scaled by a factor of 0.9 to correct for the systematic overestimation at this level of theory.[35]

[a] Present address: Lorentzian, Inc., 127 Washington Ave., North Haven, CT 06473.

 0021-9606/92/021137-13$06.00

Using the optimized geometries at the HF/6-31G* level, electron correlation effects were then calculated by means of complete fourth-order Møller–Plesset perturbation theory[36] using the 6-31G* basis set (MP4/6-31G*). This level of theory has contributions from single, double, triple, and quadruple excitations from the starting HF wave function. In order to obtain more reliable relative energies, additional calculations were carried out for all the low-energy isomers with the quadratic configuration interaction technique including corrections for triple excitations [QCISD(T)].[37] This technique is known to be accurate even for difficult systems where electron correlation effects are extremely important.[38]

Larger basis set effects were also explored for all the clusters. For the diatomic systems AlP and MgS, these were investigated at the QCISD(T)/[7*s*,6*p*,3*d*,1*f*] level, where the basis set was obtained by augmenting McLean and Chandler's 6*s*,5*p* contracted basis set[39] with a set of diffuse *sp* functions, three sets of *d* functions, and a set of *f* functions.[40] This level of theory is expected to yield the binding energies of these molecules within 0.1–0.15 eV.[12,20] In addition, all clusters were treated in a uniform manner by performing second-order Møller–Plesset perturbation (MP2) calculations with a [6*s*,5*p*,2*d*,1*f*] basis set. The larger basis set effects derived from these calculations have been used in the intercomparisons between different sized clusters. Finally, for the two lowest energy Al_3P_3 structures, we optimized the geometry at the MP2/6-31G* level and performed MP2 calculations using the [7*s*,6*p*,3*d*,1*f*] basis set at these geometries.

The atomic charges and the valence orbital hybridizations for the low energy clusters have been calculated using natural population analysis.[41–43] This method, unlike Mulliken population analysis which substantially underestimates the ionicity of molecules involving large electronegativity differences, gives a reasonable physical picture of the charge contribution while being relatively insensitive to the basis set size.[42,43]

RESULTS AND DISCUSSION

Table I lists the MP*n*/6-31G* energies [and the QCISD(T) energies when available] for the Al_nP_n clusters studied. Table II contains the analogous results for the Mg_nS_n clusters. The HF and MP2 energies using the [6*s*,5*p*,2*d*,1*f*] basis set for the low-energy isomers of Al_nP_n and Mg_nS_n, $n = 1$–3 are listed in Table III.

The effect of larger basis sets can be derived from Tables I–III and are listed as Δ(basis set) in Tables I and II. These have been obtained from the difference in energy between the MP2/[6*s*,5*p*,2*d*,1*f*] and the MP2/6-31G* results. It is clear from Tables I and II that the effects of larger basis sets are very important. The scaled HF/6-31G* zero-point energies are also given in Tables I and II. In the rest of the manuscript, unless otherwise indicated, relative energies refer to those obtained at the QCISD(T)/6-31G* level and corrected for larger basis set effects and zero-point energy corrections.

The HF/6-31G* harmonic vibrational frequencies (not scaled) are given in Table IV for the low-energy structures. Vibrational frequencies for the rest of the clusters are available from the authors. Table V gives the valence orbital configuration (i.e., 3*s* and 3*p* hybridization) for the lowest energy clusters.

All molecular structures illustrated in this work have been computer generated and drawn to scale. We represent aluminum and magnesium atoms by dark spheres and phosphorus and sulfur atoms by white spheres. In these structures, solid lines are drawn to represent internuclear dis-

TABLE I. Total energies (hartrees and kcal/mol) for aluminum phosphide clusters.

Cluster	Structure	Point group	Total energy (hartrees)[a] HF	MP2	MP3	MP4	QCISD(T)	Δ(Basis set)[b] (kcal/mol)	ZPE[c] (kcal/mol)
Al			−241.856 98	−241.886 25	−241.895 96	−241.899 51	−241.901 40	−14.4	0.0
P			−340.690 20	−340.746 89	−340.760 23	−340.763 33	−340.763 76	−26.0	0.0
AlP	a1	$C_{\infty v}$	−582.585 43	−582.692 35	−582.715 86	−582.724 01	−582.727 70	−48.6	0.5
Al_2P_2	a2	D_{2h}	−1165.243 00	−1165.563 03	−1165.588 98	−1165.616 59	−1165.618 01	−113.4	2.3
Al_2P_2	a3	D_{2h}	−1165.190 35	−1165.512 92	−1165.535 02	−1165.563 74	−1165.566 16	−117.9	3.3
Al_3P_3	a4	D_{3h}	−1747.929 36	−1748.413 60	−1748.444 95	−1748.484 12	−1748.484 94	−174.2	5.3
Al_3P_3	a7	C_s	−1747.893 42	−1748.402 94	−1748.424 11	−1748.477 32	−1748.474 00	−188.8	4.1
Al_3P_3	a11	C_s	−1747.873 26	−1748.403 21	−1748.418 89	−1748.474 40	−1748.469 86	−179.6	5.0
Al_3P_3	a5	C_s	−1747.857 81	−1748.355 97	−1748.384 90	−1748.434 37			3.9
Al_3P_3	a6	C_{2v}	−1747.880 64	−1748.389 62	−1748.409 59	−1748.464 10			3.7
Al_3P_3	a8	C_{2v}	−1747.852 06	−1748.394 46	−1748.403 68	−1748.467 55			4.1
Al_3P_3	a9	C_{2v}	−1747.826 61	−1748.370 43	−1748.380 32	−1748.445 45			4.4
Al_3P_3	a10	C_s	−1747.858 16	−1748.383 34	−1748.403 47	−1748.459 51			4.3
Al_3P_3	a12	C_1	−1747.865 53	−1748.378 85	−1748.401 66	−1748.455 21			4.4
Al_3P_3	a13	C_s	−1747.862 62	−1748.373 26	−1748.399 14	−1748.450 44			4.3
Al_3P_3	a14	C_s	−1747.871 60	−1748.369 39	−1748.399 21	−1748.447 97			4.3

[a] Calculated with the 6-31G* basis set using HF 6-31G* geometries.
[b] Larger basis set effects calculated from Table III.
[c] Zero-point energies at the HF/6-31G* level scaled by 0.9.

TABLE II. Total energies (hartrees and kcal/mol) for magnesium sulfide clusters.

Cluster	Structure	Point group	Total energy (hartrees)[a] HF	MP2	MP3	MP4	QCISD(T)	Δ (Basis set)[b] (kcal/mol)	ZPE[c] (kcal/mol)
Mg			− 199.595 61	− 199.617 60	− 199.624 77	− 199.627 38	− 199.629 17	− 7.6	0.0
S			− 397.475 96	− 397.553 38	− 397.568 14	− 397.571 47	− 397.572 29	− 38.0	0.0
MgS	b1	$C_{\infty v}$	− 597.079 95	− 597.236 88	− 597.245 58	− 597.260 97	− 597.261 86	− 57.6	0.7
Mg_2S_2	b2	D_{2h}	− 1194.359 99	− 1194.657 82	− 1194.681 12	− 1194.695 70	− 1194.697 60	− 117.1	2.9
Mg_2S_2	b3	C_{2v}	− 1194.224 63	− 1194.570 64	− 1194.594 82	− 1194.619 24	− 1194.619 16	− 118.8	2.5
Mg_2S_2	b4	C_{2v}	− 1194.298 01	− 1194.576 76	− 1194.599 25	− 1194.613 41	− 1194.615 56	− 117.5	2.4
Mg_3S_3	b5	D_{3h}	− 1791.628 38	− 1792.077 52	− 1792.113 03	− 1792.133 76	− 1792.135 89	− 171.3	4.6
Mg_3S_3	b6	C_1	− 1791.387 87	− 1791.843 10	− 1791.855 16	− 1791.913 53	− 1791.918 58	− 182.3	3.9
Mg_3S_3	b7	C_1	− 1791.480 38	− 1791.949 65	− 1791.984 73	− 1792.012 70	− 1792.015 92	− 178.6	4.1

[a] Calculated using HF/6-31G* geometries.
[b] Larger basis set effects calculated from Table III.
[c] Zero-point energies at the HF/6-31G* level scaled by 0.9.

tances that are within 15% of the bulk bond lengths. While most of the interesting geometrical parameters are shown in the figures, the rest are available from the authors. The atomic charges calculated from the natural population analysis are also shown adjacent to the respective atoms in all figures.

Aluminum phosphide clusters

In this section, we discuss our results for diatomic AlP and the different structures of Al_2P_2 and Al_3P_3.

AlP

The diatomic aluminum phosphide molecule (a1) has a $^3\Sigma^-$ ground state. This electronic state which contains two π electrons is analogous to the corresponding ground state of the isoelectronic Si_2 molecule. The optimized HF/6-31G* bond length is 2.43 Å, somewhat larger than the bulk Al–P bond length of 2.36 Å.[44] We also investigated the $^3\Pi$ state which is known to be low lying for Si_2. It has a bond length of 2.27 Å, the shorter distance being consistent with having three π electrons. The energy difference between the two states is 11.8 kcal/mol at the HF/6-31G* level. Including the correlation energy at the QCISD(T)/[7*s*,6*p*,3*d*,1*f*] level makes the $^3\Sigma^-$ only 1.2 kcal/mol more stable than the $^3\Pi$ state. This is very similar to the value calculated by Meier *et al.*[45] and is also very close to the energy difference found between the analogous states in Si_2.[12] On the other hand, the corresponding states in GaAs appear to be split by a larger amount.[22,25,29]

TABLE III. Calculated energies (hartree) for aluminum phosphide and magnesium sulfide clusters with HF/6-31G* geometries using the [6*s*,5*p*,2*d*,1*f*] basis set.

Cluster	Structure	Point group	[6*s*,5*p*,2*d*,1*f*] Basis set HF	MP2
Al			− 241.873 70	− 241.909 13
P			− 340.707 33	− 340.788 25
AlP	a1	$C_{\infty v}$	− 582.624 68	− 582.769 82
Al_2P_2	a2	D_{2h}	− 1165.333 47	− 1165.743 75
Al_2P_2	a3	D_{2h}	− 1165.283 87	− 1165.700 73
Al_3P_3	a4	D_{3h}	− 1748.066 34	− 1748.691 19
Al_3P_3	a7	C_s	− 1748.038 09	− 1748.703 75
Al_3P_3	a11	C_s	− 1748.010 86	− 1748.689 50
Mg			− 199.606 56	− 199.629 64
S			− 397.501 35	− 397.613 95
MgS	b1	$C_{\infty v}$	− 597.121 50	− 597.328 73
Mg_2S_2	b2	D_{2h}	− 1194.444 28	− 1194.844 41
Mg_2S_2	b3	C_{2v}	− 1194.313 78	− 1194.759 97
Mg_2S_2	b4	C_{2v}	− 1194.386 53	− 1194.763 93
Mg_3S_3	b5	D_{3h}	− 1791.752 77	− 1792.350 55
Mg_3S_3	b6	C_1	− 1791.522 13	− 1792.133 62
Mg_3S_3	b7	C_1	− 1791.610 09	− 1792.234 29

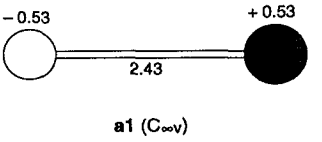

a1 ($C_{\infty v}$)

Natural population analysis yields atomic charges of + 0.53*e* on Al and − 0.53*e* on P, consistent with the electronegativity difference between the elements. Since both Al and P are trivalent elements, the atomic charges of only $\simeq$0.5*e* indicate significant covalent contribution to the bonding.

As a calibration of the accuracy of our calculations, we compare the calculated binding energy of AlP with the known experimental value of 2.2 eV.[46] At the QCISD(T)/6-31G* level of theory, the calculated value (1.70 eV) is significantly smaller than the experimental value. Inclusion of the effect of larger basis sets at the QCISD(T)/[7*s*,6*p*,3*d*,1*f*] level increases the binding energy to 2.07 eV, in excellent agreement with the experiment. If we include the larger basis set effect at the MP2 level with the smaller [6*s*,5*p*,2*d*,1*f*] basis set, an almost identical value of 2.06 eV is obtained (Table I). Thus Δ(basis set) values listed in Tables I and II describe the larger basis set effects reliably.

TABLE IV. The harmonic vibrational frequencies calculated at the HF/6-31G* level.

Cluster	Structure	Point group	Vibrational frequencies (cm^{-1})
AlP	a1	$C_{\infty v}$	$381(\sigma_g)$
Al_2P_2	a2	D_{2h}	$96(b_{3u})$, $149(b_{2u})$, $239(b_{3g})$, $280(a_g)$, $353(b_{1u})$, $644(a_g)$
Al_2P_2	a3	D_{2h}	$185(b_{3u})$, $341(b_{3g})$, $348(b_{2u})$, $409(a_g)$, $509(a_g)$, $525(b_{1u})$
Al_3P_3	a4	D_{3h}	$121(e'')$, $163(a_2'')$, $221(e')$, $340(a_1')$, $360(e')$, $403(a_1')$, $541(a_2')$, $631(e')$
Al_3P_3	a7	C_s	$49(a'')$, $79(a')$, $125(a')$, $140(a'')$, $197(a')$, $210(a'')$, $252(a')$, $304(a')$, $388(a')$, $415(a'')$, $451(a')$, $551(a')$
Al_3P_3	a11	C_s	$85(a'')$, $201(a'')$, $227(a')$, $259(a'')$, $286(a')$, $317(a')$, $333(a'')$, $340(a')$, $407(a')$, $451(a'')$, $464(a')$, $538(a')$
Al_3P_3	a5	C_s	$8i(a'')$, $45(a')$, $78(a'')$, $128(a')$, $170(a')$, $262(a')$, $274(a'')$, $300(a')$, $360(a')$, $421(a'')$, $471(a')$, $520(a'')$
Al_3P_3	a6	C_s	$125i(b_1)$, $53(b_2)$, $131(a_1)$, $146(b_1)$, $153(a_2)$, $160(b_2)$, $239(a_1)$, $285(a_1)$, $319(b_1)$, $415(a_1)$, $432(b_2)$, $556(a_1)$
Al_3P_3	a8	C_{2v}	$67i(b_2)$, $58i(b_1)$, $135(a_1)$, $198(a_1)$, $218(b_1)$, $277(b_2)$, $286(a_1)$, $290(a_2)$, $312(b_1)$, $378(a_1)$, $518(b_2)$, $528(a_1)$
Al_3P_3	a9	C_{2v}	$164i(b_2)$, $108i(b_1)$, $164(b_1)$, $204(a_1)$, $279(a_2)$, $302(a_1)$, $311(b_2)$, $339(a_1)$, $380(b_1)$, $447(a_1)$, $481(a_1)$, $521(b_2)$
Al_3P_3	a10	C_s	$69(a'')$, $84(a')$, $141(a'')$, $194(a')$, $219(a'')$, $245(a')$, $280(a'')$, $298(a')$, $352(a')$, $401(a')$, $440(a')$, $599(a')$
Al_3P_3	a12	C_1	51, 104, 143, 184, 219, 265, 274, 355, 382, 449, 493, 525
Al_3P_3	a13	C_s	$103i(a'')$, $74(a')$, $156(a'')$, $196(a'')$, $220(a')$, $237(a')$, $281(a')$, $354(a'')$, $376(a')$, $457(a')$, $477(a'')$, $539(a')$
Al_3P_3	a14	C_s	$27(a'')$, $58(a')$, $130(a'')$, $154(a')$, $204(a'')$, $246(a')$, $302(a'')$, $312(a')$, $411(a')$, $421(a'')$, $475(a')$, $582(a')$
MgS	b1	$C_{\infty v}$	$539(\sigma_g)$
Mg_2S_2	b2	D_{2h}	$178(b_{3u})$, $305(a_g)$, $363(b_{2u})$, $392(b_{3g})$, $459(a_g)$, $513(b_{1u})$
Mg_2S_2	b3	C_{2v}	$110(a_2)$, $218(b_1)$, $235(a_1)$, $268(b_2)$, $390(a_1)$, $500(a_1)$
Mg_3S_3	b5	D_{3h}	$107(e')$, $140(e')$, $166(a_2'')$, $258(a_1')$, $332(a_1')$, $342(e')$, $515(a_2')$, $553(e')$
Mg_3S_3	b6	C_1	54, 80, 123, 139, 148, 239, 251, 272, 298, 375, 502, 541
Mg_3S_3	b7	C_1	83, 98, 175, 202, 204, 236, 241, 299, 343, 379, 460, 497

Al_2P_2

The lowest energy structure containing two Al and two P atoms is a rhombus with the phosphorus atoms along the short diagonal. This D_{2h} structure is labeled a2 and has a ^1A_g ground state. If the molecule is in the yz plane with the y axis along the short diagonal, the valence electron configuration is $(a_g)^2(b_{2u})^2(b_{1u})^2(a_g)^2(b_{3u})^2(a_g)^2(b_{3g})^2(b_{1u})^2$. Here b_{3u} is a bonding π orbital and the remaining orbitals correspond to the radial and tangential σ-bonding combinations. Both the rhombus geometry and the orbital configuration are exactly analogous to that of the isoelectronic Si_4 molecule[12] and the valence-isoelectronic Ga_2As_2.[25] However, the strong P–P bonding in Al_2P_2 differs from the rather

TABLE V. Valence natural orbital configurations[a] for the different atoms calculated at the HF/6-31G* level.

AlP clusters					MgS clusters				
Cluster	Structure	Point group	Atom(s)	Hybridization	Cluster	Structure	Point group	Atom(s)	Hybridization
AlP	a1	$C_{\infty v}$	Al	$s^{1.88}p^{0.55}$	MgS	b1	$C_{\infty v}$	Mg	$s^{0.65}p^{0.10}$
			P	$s^{1.93}p^{3.58}$				S	$s^{1.97}p^{5.25}$
Al_2P_2	a2	D_{2h}	Al	$s^{1.87}p^{0.50}$	Mg_2S_2	b2	D_{2h}	Mg	$s^{0.37}p^{0.03}$
			P	$s^{1.74}p^{3.82}$				S	$s^{1.95}p^{5.57}$
Al_2P_2	a3	D_{2h}	Al	$s^{0.87}p^{0.96}$	Mg_2S_2	b3	C_{2v}	Mg	$s^{1.08}p^{0.03}$
			P	$s^{1.77}p^{4.30}$				S	$s^{1.93}p^{4.89}$
Al_3P_3	a4	D_{3h}	Al	$s^{0.77}p^{1.02}$	Mg_3S_3	b5	D_{3h}	Mg	$s^{0.34}p^{0.03}$
			P	$s^{1.71}p^{4.41}$				S	$s^{1.94}p^{5.62}$
Al_3P_3	a7	C_s	Al_1	$s^{1.84}p^{0.63}$	Mg_3S_3	b6	C_1	Mg_1	$s^{1.42}p^{0.27}$
			Al_2	$s^{1.86}p^{0.46}$				Mg_2	$s^{1.50}p^{0.10}$
			Al_3	$s^{1.65}p^{0.74}$				Mg_3	$s^{0.84}p^{0.12}$
			P_1	$s^{1.71}p^{3.65}$				S_1	$s^{1.88}p^{4.83}$
			P_2, P_3	$s^{1.71}p^{3.88}$				S_2	$s^{1.77}p^{4.30}$
								S_3	$s^{1.87}p^{4.90}$
Al_3P_3	a11	C_s	Al_1	$s^{0.93}p^{1.20}$	Mg_3S_3	b7	C_1	Mg_1	$s^{0.31}p^{0.03}$
			Al_2, Al_3	$s^{1.24}p^{0.96}$				Mg_2	$s^{1.01}p^{0.08}$
								Mg_3	$s^{1.01}p^{0.08}$
			P_1	$s^{1.72}p^{4.27}$				S^1	$s^{1.97}p^{5.63}$
			P_2, P_3	$s^{1.71}p^{3.90}$				S_2	$s^{1.88}p^{4.90}$
								S_3	$s^{1.88}p^{4.90}$

[a] Contributions from $4s$, $3d$, and $4p$ are very small (<0.05) and will be ignored.

weak Si–Si bonding across the short diagonal in Si_4. As shown in the figure, the Al–Al, P–P, and Al–P interatomic distances in a2 are 4.64, 2.04, and 2.53 Å, respectively. The Al–P–Al angle is 132° and the P–Al–P angle is 48°. Natural population analysis yields atomic charges of $\pm 0.61e$, showing slightly larger charge separation than in diatomic AlP.

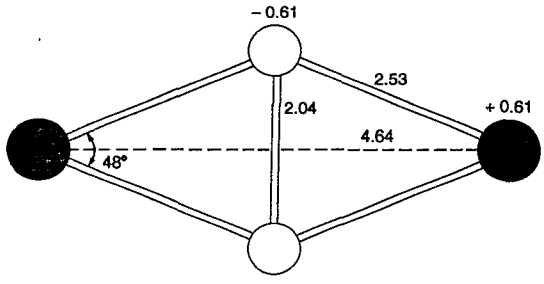

a2 (D_{2h})

A second rhombic structure, shown here as a3, is also possible for Al_2P_2 with the aluminum atoms occupying the short diagonal. As given in Table I, a3 is 39 kcal/mol higher in energy than a2. a3 also has D_{2h} symmetry and a ^1A_g electronic state. However, the orbital configuration is different—$(a_g)^2(b_{1u})^2(a_g)^2(b_{2u})^2(b_{3u})^2(b_{3g})^2(b_{1u})^2(b_{2g})^2$. In a3, the Al–Al, P–P, and Al–P distances are 2.37, 3.87, and 2.27 Å, respectively. The Al–P–Al angle is 63° and the P–Al–P angle is 117°. Both a2 and a3 are found to be minima, as seen from the vibrational frequencies listed in Table IV.

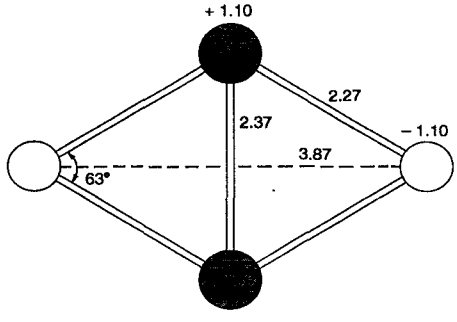

a3 (D_{2h})

The bonding in a3 is highly ionic with atomic charges of $\pm 1.10e$. The high degree of ionic character is consistent with the fact that the orbital configuration in a3 is analogous to that in the more ionic Mg_2S_2 (*vide infra*) and the almost completely ionic Na_2Cl_2 molecule.[28] We noted earlier that the orbital configuration in a2 is analogous to the more covalent Si_4 structure. Thus the two different rhombus forms a2 and a3 have electronic configurations which are governed principally by covalent and ionic bonding contributions. The extra stability of a2 over a3 could be attributed to the formation of a strong covalent bond between the phosphorus atoms in a2. The hybridization and bonding in these structures is considered in more detail in a later section. Other structures such as linear forms are found not to be competitive with the rhombus ground state.

Al_3P_3

The number of different isomers that can be formed from a mixed cluster is large. This arises not only from the many different geometric possibilities, but also from the different permutations of the two atoms which are possible in a mixed cluster within a given geometry. We have considered several possible candidates for the ground state structure of Al_3P_3 and have identified a rich and varied set of local minima. First, we consider planar structures which are suggested by electrostatic considerations and then the three-dimensional forms suggested by analogy with isoelectronic Si_6.

The lowest energy planar structure (a4) has D_{3h} symmetry. In this structure, the three phosphorus atoms are edge capping the triangle formed from the three aluminum atoms. The optimized Al–Al and Al–P internuclear distances in a4 are 2.85 and 2.21 Å, respectively. The Al–P–Al angle is 80°. The Al–Al distance in a4 is very close to that in bulk Al (2.86 Å),[44] but the Al–P bond length is 0.15 Å shorter than the bulk value of 2.36 Å.[44] As shown in Table I, a4 is the lowest energy structure at the MP4/6-31G* and QCISD(T)/6-31G* levels. Including the effects of larger basis sets makes a4 slightly less stable than one of the three-dimensional structures (*vide infra*). In a4, the atomic charges are $\pm 1.14e$, indicating the highly ionic character of this two-dimensional structure. This is comparable to the atomic charges in the ionic form of Al_2P_2 (a3) seen earlier. The orbital configuration and geometry of a4 are analogous to that in the ionic systems Na_3Cl_3 and Mg_3S_3.

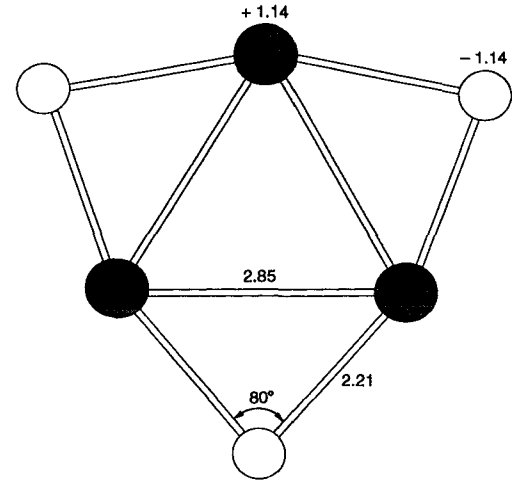

a4 (D_{3h})

To find out the importance of the specific atomic arrangements in a4, we also studied the other planar D_{3h} structure, where the aluminum atoms cap the phosphorus triangle (structure not shown). The optimized geometry for such a structure shows a P–P bond length of 2.22 Å and an Al–P bond length of 2.59 Å. The P–Al–P angle is 51°. This structure is 88 kcal/mol higher in energy than a4 at the MP4/6-31G* level. However, vibrational frequency analysis shows that it has two imaginary frequencies—a degenerate e'' of $519i$ cm^{-1} and another a_2' frequency of $180i$ cm^{-1}. This indicates that further stabilization is possible for both in-

plane and out-of-plane symmetry breaking distortions.

Relaxing the symmetry to a planar C_s arrangement leads to a benzenelike structure (a5). This structure lies 30 kcal/mol above a4 at the MP4/6-31G* level. Vibrational frequency analysis indicates that the molecule still has a small a'' imaginary frequency of $8i$ cm^{-1}. It is unlikely that significant energy lowering can be obtained by further distortion since the potential surface is obviously very shallow. As shown in a5, there are no Al–Al bonds in this structure, but there are two P–P bonds (2.22 Å) and seven Al–P bonds having bond lengths of 2.27, 2.53, 2.63, and 2.75 Å.

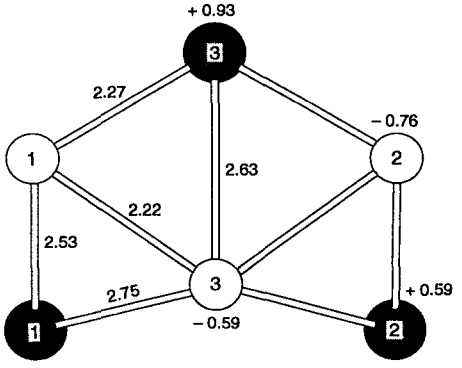

a5 (C_s)

Previous detailed studies on silicon clusters have shown that the ground state structure of isoelectronic Si_6 is an edge-capped trigonal bipyramid with C_{2v} symmetry.[12] We have thus considered the geometry of Al_3P_3 with a similar structure. However, the presence of two different types of atoms in Al_3P_3 leads to several isomeric structures. In particular, we have identified two low-energy isomers based on the Si_6-like geometry, which we discuss in detail.

Among the Si_6-like structures considered, one of the low-lying C_{2v} forms (a6) corresponds to an aluminum atom edge-capping two neighboring phosphorus atoms as shown below.

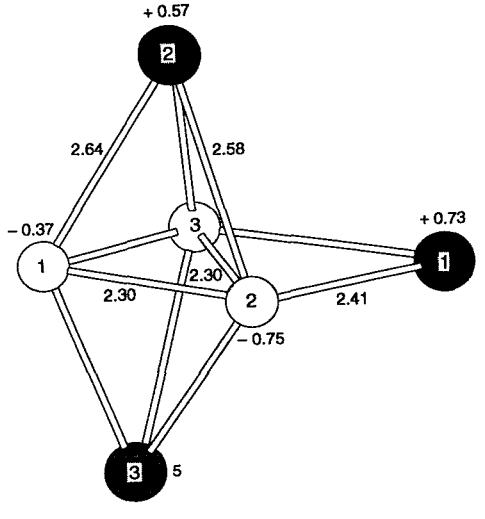

a6 (C_{2v})

This structure can be derived from an analysis of the charge distribution on the different atoms (typically ranging from ± 0.1–$0.3e$) in the ground state of Si_6 structure. a6 corresponds to replacing the three silicon atoms with the largest partial negative charges with P and the remaining atoms with Al. At the zero-point corrected MP4/6-31G* level, a6 is 11 kcal/mol higher in energy than the planar D_{3h} form considered earlier. However, it has an imaginary frequency $125i(b_1)$, suggesting that distortion to C_s symmetry can lead to lower energy.

The resulting C_s structure (a7) is a local minimum. The geometry of a7 is interesting with a range of Al–P distances between 2.35 and 2.91 Å. Clearly, the concept of a traditional covalent bond is not valid for these mixed clusters. The interplay between partial covalent bonds and partial ionic bonds (again involving a range of partial charges) can yield a broad range of internuclear distances between Al and P. However, the P–P distances show only a small range (2.21–2.24 Å) clearly indicating P–P covalent bonds. The only Al–Al bond (2.85 Å) is also very close to the bulk distance of 2.86 Å. Natural population analysis yields charges of $+0.50$, $+0.65$, and $+0.57e$ for Al_1, Al_2, and Al_3, respectively. P_1 has a charge of $-0.42e$, while the equivalent atoms P_2 and P_3 have a charge of $-0.65e$. The presence of a larger partial negative charge on P_2 and P_3 is clearly related to the fact that they are closer to more aluminum atoms than P_1.

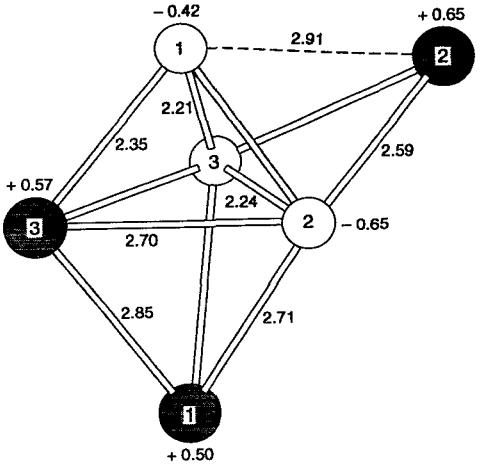

a7 (C_s)

a7 is comparable in stability to the planar ionic from a4. At the MP4/6-31G* level, it is 3 kcal/mol less stable than a4. The inclusion of larger basis set effects reverses the stability (*vide infra*) and at the higher levels of theory, a7 is more stable than all other structures considered and appears to be the ground state of Al_3P_3.

We also optimized a C_s structure similar to a7, except for interchanging the positions of Al_3 and P_2 (structure not shown). Vibrational frequency analysis yields an imaginary frequency of $76i(a'')$. Further relaxation leads to a C_1 structure that is 18 kcal/mol less stable than a7. The two analogous Ga_3As_3 structures have a similar energy difference (*13* kcal/mol).[29]

Another Si_6-like structure (a8) is a different C_{2v} form which corresponds to an aluminum atom capping the two other aluminum atoms as shown below.

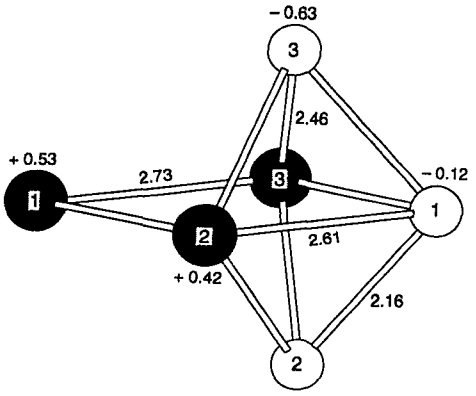

a8 (C_{2v})

At the HF/6-31G* level, a8 is significantly less stable than a6 considered earlier. However, after the inclusion of electron correlation effects, the ordering is reversed with a8 being 2 kcal/mol more stable than a6. However, a8 has two imaginary frequencies $67i(b_2)$ and $58i(b_1)$ again indicating distortion to C_1 symmetry.

We have studied the symmetry breaking pathways very carefully. One of them leads to a saddle point with one imaginary frequency, while the other leads to a true minimum. In the latter pathway, one of the Al–Al bonds in a8 is completely broken while maintaining the equivalence of P_2 and P_3. This eventually ends up in a C_s structure which is identical to a7 considered earlier. Thus, two seemingly different forms (a6 and a8) lead to the same local minimum. This demonstrates clearly the richness of the potential energy surface for mixed clusters and the complex interconnections between the different isomers.

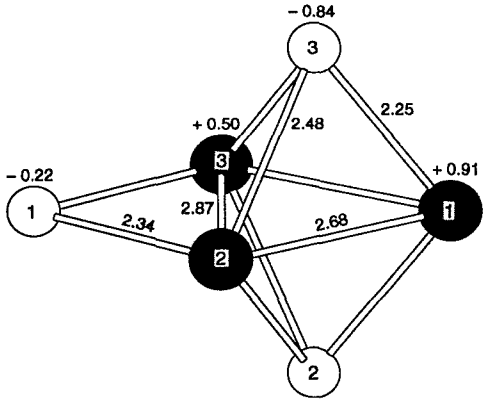

a9 (C_{2v})

We also optimized a third Si_6-like isomer (a9) where a P atom caps an Al–Al edge. As in a6, vibrational analysis indicates the presence of two imaginary frequencies $164i(b_2)$ and $108i(b_1)$. On distortion to C_s symmetry, a local minimum structure (a10) is obtained. The distortion migrates P_1 to form a bond with one of the other phosphorus atoms while maintaining the equivalence of Al_2 and Al_3. The Al–P distances show a smaller range of values between 2.20 and 2.46 Å, while the Al–Al distances vary from 2.90 to 3.06 Å, slightly larger than the bulk distance of 2.86 Å. a10 is 14 kcal/mol higher in energy than a4 at the MP4/6-31G* level. The atoms Al_1 and P_3 have larger charges than the other atoms.

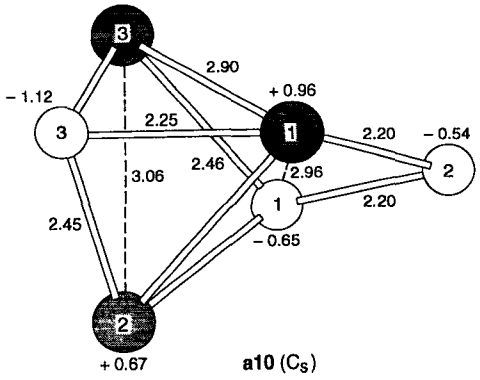

a10 (C_S)

Another structure which we have considered in detail is the trigonal prism. While it is not a low-energy structure for Si_6, it appears to be particularly suited to trivalent elements such as Al and P since each corner of a trigonal prism has a coordination number of three. Again, since there are two different types of elements, several isomers are possible. We describe some of the low-energy isomers in this section.

The lowest energy trigonal-prismlike structure is shown below as a11 with C_s symmetry. Here one of the triangles is made of two phosphorus and one aluminum atoms, while the other is made of one phosphorus and two aluminum atoms. The optimized structure has the two opposite triangles positioned such that a pair of additional Al–Al "bonds" are formed (labeled as Al_1–Al_2 and Al_1–Al_3). The Al–Al distances vary from 2.55–2.82 Å, while the Al–P distances vary from 2.29–2.40 Å. The only bonded P–P distance 2.36 Å is significantly larger than the typical P–P bond length of $\simeq$2.20 Å.[44] An alternative way of considering this structure is that it has a triangle of aluminum atoms which are capped on one side by P_1 and on the other side by P_2 and P_3, which are also bonded to each other. a11 is a local minimum which lies only 6 kcal/mol higher in energy that a4 at the MP4/6-31G* level.

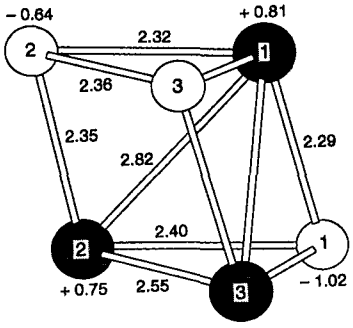

a11 (C_S)

The partial charges on the phosphorus atoms P_1 and $P_{2,3}$ are -1.02 and $-0.64e$, respectively, while the aluminum atoms Al_1 and $Al_{2,3}$ have charges of $+0.81$ and $+0.75e$, respectively. As shown in a11, P_1 and Al_1 are more ionic than the other phosphorus and aluminum atoms and their interatomic distances are shorter.

Another possibility exists for connecting a triangle made of two Al and one P atom with another triangle made of one P and two Al atoms. In such structure, instead of the like atoms being arranged in a staggered manner as in a11, they are arranged to form additional bonds between like atoms. Thus, a starting configuration for such a structure has five Al–P bonds, two Al–Al bonds, and two P–P bonds. Optimizing this structure eventually led to a local minimum a12 (C_1 symmetry).

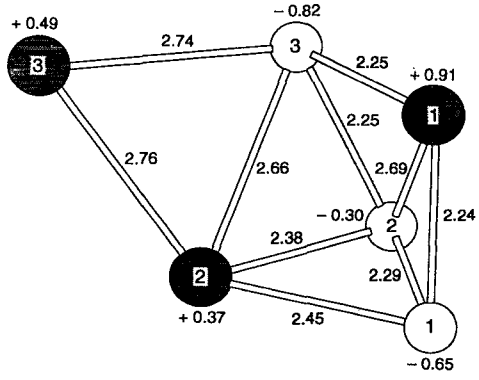

a12 (C_1)

However, the final geometry does not resemble the starting geometry at all with many bonds being broken. a12 is 17 kcal/mol higher in energy than a4 at the zero-point corrected MP4/6-31G* level of theory. The Al–P bond lengths vary from 2.24 to 2.74 Å, again showing a substantial range, while the Al–Al bond length is 2.76 Å and the P–P distances are 2.25 and 2.29 Å.

The atomic charges on the atoms vary considerably, depending on their location. Al_1, which is surrounded by three phosphorus atoms, has a charge of $+0.91e$. On the other hand, Al_2, which is surrounded by three phosphorus atoms and one other aluminum atom, has much lower atomic charge ($+0.37e$). Similar behavior is observed for the charges on the phosphorus atoms, as shown in a12.

We also considered a trigonal prism structure with C_{3v} symmetry in which each triangle is made of the same atoms (structure not shown). The aluminum atoms in such structure are 3.90 Å apart, forming a larger base than the corresponding phosphorus base which has a side length of 2.23 Å. The optimized Al–P bond length is 2.41 Å. This structure is 57 kcal/mol higher in energy than a11. It has two imaginary frequencies $135i(e)$ and $51i(a_2)$ cm^{-1} indicating that it can be further stabilized by relaxing the symmetry constrains.

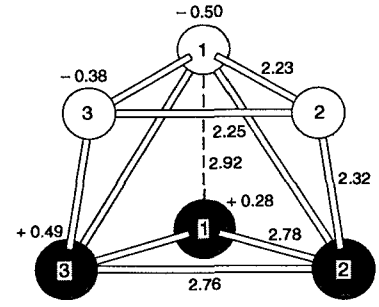

a13 (C_S)

Relaxing the symmetry to C_s leads to a13. This symmetry relaxation lowers the energy by over 40 kcal/mol, making a13 20 kcal/mol higher in energy than a4 at the MP4/6-31G* level. As shown, the P–P distances are 2.23 and 2.25 Å and the Al–P internuclear distances are 2.32 and 2.92 Å. The Al–Al internuclear distance is reduced from 3.90 Å in the C_{3v} structure to 2.78 Å in a13. Vibrational frequency analysis shows that a13 still has an imaginary frequency of $103i(a'')$ cm^{-1}. Distortion to C_1 symmetry eventually led to the more open C_s form a14. Although a14 is a local minimum at the MP4/6-31G* level, it is slightly higher in energy than a13 at the correlated MP4/6-31G* level. Thus, it is possible that a13 itself may be a minimum at the correlated levels of theory. However, both a13 and a14 are significantly higher in energy than the low-energy isomers considered earlier.

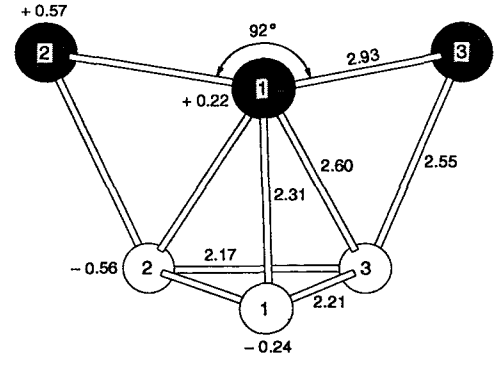

a14 (C_S)

Our relative energy comparison so far is based on the zero-point energy corrected MP4/6-31G* results. Up to this point, we determined the low-lying energy structures to be the planar form a4, the aluminum face-capped Si_6-like structure a7, and the trigonal prism a11.

We further investigated the three low energy structures to find their relative energies using more sophisticated level of theory. The total energies at the QCISD(T) level are reported in Table I. Larger basis set effects at the MP2 level calculated with the [6*s*,5*p*,2*d*,1*f*] basis sets are shown in Table III. At the MP4/6-31G* level of theory, the planar a4 is more stable than a7 and a11 by 3 and 6 kcal/mol, respectively. However, larger basis sets clearly favor the Si_6-like

structure a7 relative to the planar form a4. At the highest level, the order of stability is reversed so that a7 is more stable than the D_{3h} planar structure (a4) by 9 kcal/mol and more stable than the trigonal prism structure (a11) by 13 kcal/mol. Due to the small energy difference between a4 and a7 and the change in the order of stability with the size of the basis set, we optimized the geometries of these two structures at the MP2/6-31G* level. The optimized bond lengths at this level are slightly shorter than those at the HF/6-31G* level. Since the size of the basis set is very important, we also performed MP2 calculations using the contracted [7*s*,6*p*,3*d*,1*f*] basis set at the MP2/6-31G* optimized geometry. At this level, a7 is more stable than a4 by 6.3 kcal/mol (very similar to the results in Table I).

In addition to the singlet states considered so far, we optimized the geometries of several triplet states at the HF/6-31G* level. Triplet states derived from the abovementioned low energy structures are significantly higher in energy than the corresponding singlet states, particularly after including the effects of electron correlation.

Magnesium sulfide clusters

Magnesium sulfide clusters behave quite different from the corresponding aluminum phosphide clusters, particularly in the nature of the ground state structures. The principal reason is that due to the larger electronegativity difference between Mg and S, ionic bonding contributions are much more important for MgS clusters. This can be seen clearly in the discussion below.

MgS

Magnesium sulfide (b1) has a $^1\Sigma^+$ ground state. The Mg–S HF/6-31G* optimized bond length is 2.15 Å, in very good agreement with the dimer experimental value of 2.14 Å.[46] The energy difference between the $^1\Sigma^+$ ground state and the low-lying $^3\Pi$ state is calculated to be 8.2 kcal/mol at the QCISD(T)/[7*s*,6*p*,3*d*,1*f*] level. The $^3\Sigma^-$ state is much higher in energy. As shown in the figure, the atoms have charges of $\pm$ 1.23*e*, indicating higher ionicity than any of the AIP clusters considered in this study.

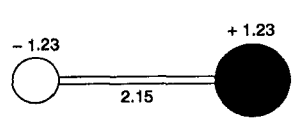

b1 ($C_{\infty v}$)

The binding energy of MgS has been calculated at the QCISD(T)/[7*s*,6*p*,3*d*,1*f*] level and yields a value of 2.08 eV. This is consistent with the results from the experimental measurements which yield an upper limit of 2.4 eV.[46]

Mg_2S_2

We considered both singlet and triplet structures with linear and rhombic geometries. Structures based on a linear geometry did not yield any low energy isomers (some of them collapsing to the rhombus structure) and are not discussed. As in the case of Al_2P_2, we explored the possibilities of having either the magnesium atoms or the sulfur atoms along the short diagonal of the rhombus.

Optimization of the rhombus structure with the Mg atoms on the short diagonal yields the lowest energy structure b2.

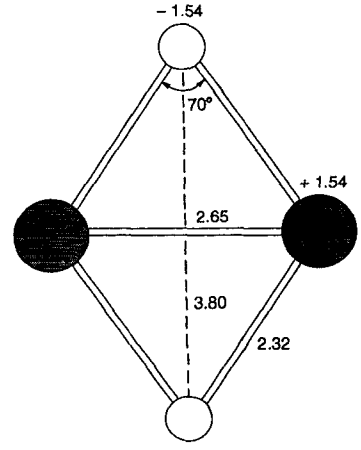

b2 (D_{2h})

This structure is very similar to the Al_2P_2 structure a3 considered earlier. It has D_{2h} symmetry and ^1A_g ground state with the valence electronic configuration $(a_g)^2\,(b_{1u})^2\,(a_g)^2\,(b_{2u})^2\,(b_{3g})^2\,(b_{3u})^2\,(b_{1u})^2\,(b_{2g})^2$. The Mg–S bond distance is 2.32 Å and the Mg–Mg distance is 2.65 Å.

We also considered the Mg_2S_2 rhombic structure that resembles the Al_2P_2 ground state geometry a2. For such a D_{2h} structure, both singlet and triplet low-energy forms were obtained with a ^1A_g state being 8 kcal/mol more stable than a $^3B_{1u}$ state at the MP4/6-31G* level. Vibrational frequency analysis revealed the existence of a b_{3u} imaginary frequency of 20*i* for the singlet and of 70*i* for the triplet state. These imaginary frequencies indicate out-of-plane distortions to lead to C_{2v} symmetries. Symmetry relaxation of the singlet state led to a C_{2v} structure with a $^1A_1$ ground state. Although such a symmetry relaxation lowered the HF energy of the C_{2v} structure relative to the D_{2h} structure, the correlation energy favored the D_{2h} structure. In order to characterize it further, additional MP2/6-31G* optimization of the C_{2v} form were carried out. This led to b3, a structure that is 1 kcal/mol lower in energy than the D_{2h} form at the MP4/6-31G* level. The valence orbital configuration for b3 is $(a_1)^2\,(b_2)^2\,(b_1)^2\,(a_1)^2\,(a_1)^2\,(a_2)^2\,(b_2)^2\,(a_1)^2$. As shown below, the S–S, Mg–Mg, and S–Mg internuclear distances are 2.27, 4.24, and 2.44 Å, respectively. The Mg–S–Mg angle is 121°.

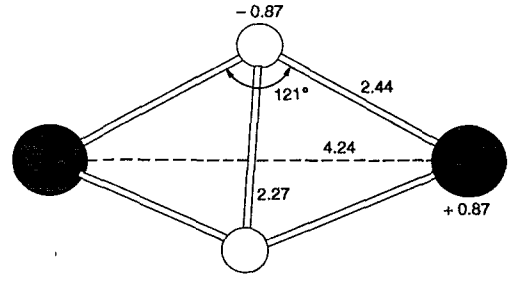

b3 (C_{2v})

Symmetry relaxation of the $^3B_{1u}$ state led to b4, which is 5 kcal/mol lower in energy than the parent D_{2h} structure. b4 ($^3B_1$ state) has the valence electronic configuration $(a_1)^2$ $(b_2)^2$ $(b_1)^2$ $(a_1)^2$ $(a_1)^2$ $(a_2)^2$ $(b_2)^2$ $(a_1)^1$ $(b_1)^1$. In this structure, the S–S and Mg–Mg internuclear distances (2.19 and 3.83 Å, respectively) are shorter than the corresponding distances in b3. The Mg–S distance, on the other hand, is slightly longer. The Mg–S–Mg angle in b4 is 20° smaller than that in b3. A puckered triplet structure similar to b4 has been seen previously for Si_4.[12]

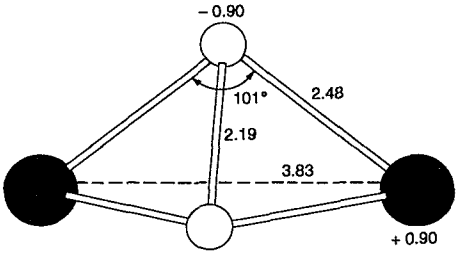

b4 (C_{2v})

As shown in Table II, b3 and b4 are close in energy. After including the effects of larger basis sets using MP2/[6*s*,5*p*,2*d*,1*f*] calculations, b3 is only 3.5 kcal/mol more stable than b4. However, as shown in Table II, both b3 and b4 are much higher in energy than the ground state structure b2.

Atoms in b3 and b4 have charges of $\pm 0.87e$ and $\pm 90e$, respectively. These are much smaller than the charges of ± 1.54 seen for b2. Thus, in the two-dimensional structure b2, charge alternation can be more effectively utilized than in the three-dimensional structures b3 and b4. From Table II, b2 is 47 kcal/mol lower in energy than b3 at the highest level of theory. This is the reverse of the ordering found for Al_2P_2 and shows the importance of ionic bonding in Mg_2S_2, while covalent bonding is more important for Al_2P_2 (and Si_4).

Mg_3S_3

To find the low-lying energy structures of Mg_3S_3, we started with geometries similar to those in the low energy structures in Al_3P_3. Since ionic terms are more important for MgS, we first started with a planar D_{3h} structure for Mg_3S_3. This structure, labeled b5, shows the sulfur atoms edge capping the magnesium atom triangle. Our calculations show that the ground state is a singlet, similar to that in the Al_3P_3 case. The Mg–Mg interatomic distance is 3.30 Å and the Mg–S interatomic distance is 2.29 Å. The Mg–S–Mg bond angle is 92°. The Mg–Mg bond distance is close to the bulk value of 3.20,[44] but the Mg–S bond length is shorter than the bulk value of 2.6.[47] As shown in b5, the natural charges on the atoms are $\pm 1.58e$ and are comparable to those in b2. This is a clear indication of the high ionic character of b5.

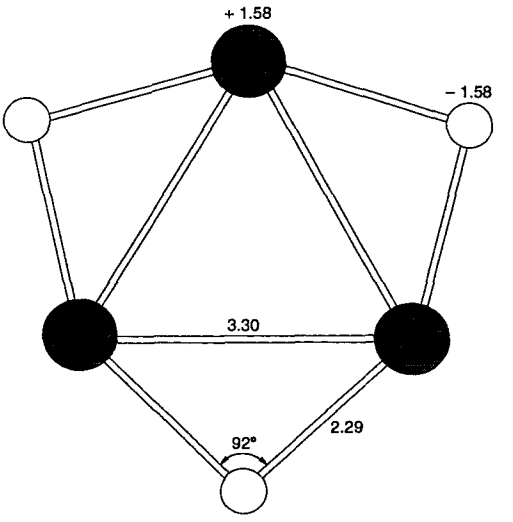

b5 (D_{3h})

We also optimized the geometry of the C_s structure that resembles the Si_6-like form a7. However, vibrational frequency analysis for the analogous Mg_3S_3 shows that this structure is not a local minimum. Further relaxation led to a structure that has no symmetry, labeled b6, and does not show much resemblance to the starting Si_6-like structure. This seems to be due to the geometrical relaxation toward a planar structure. Although a7 is the lowest-energy form for Al_3P_3 cluster, b6 is 137 kcal/mol higher in energy than b5 at the MP4/6-31G* level.

As shown in b6, the Mg–Mg bond lengths are 3.48, 2.84, and 2.98 Å. The S–S bond lengths are 2.10 Å and the Mg–S bond lengths are 2.42, 2.69, and 2.52 Å. The natural charges in b6 change with the position of the atom in the molecule. The magnesium atoms labeled Mg_1 and Mg_2 have charges of $+0.30$ and $+0.38e$, respectively, reflecting their covalent nature. The other magnesium atom (Mg_3) has a charge of $+1.01e$. The charges on the sulfur atoms are -0.74, -0.13, and $-0.82e$.

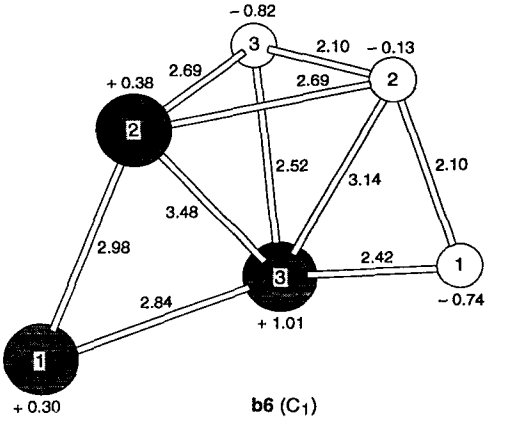

b6 (C_1)

Since the trigonal-prismlike structure a11 is a low-lying energy form for Al_3P_3, we optimized the analogous Mg_3S_3 structure. The vibrational frequency analysis of this C_s structure at the HF/3-21G* level shows that it has an imagi-

nary frequency of $65i(a'')$. However, the resulting C_1 distortion was rather small and led to the structure b7. This trigonal-prismlike structure is 75 kcal/mol higher in energy than the planar structure b5 at the MP4/6-31G* level.

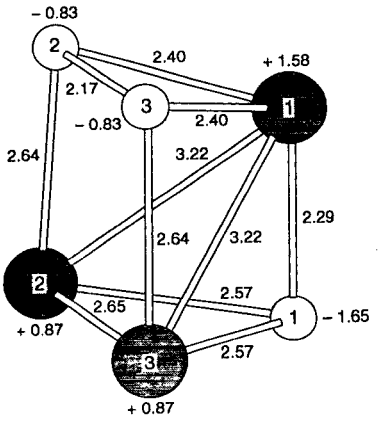

b7 (C_1)

The atoms in b7 have larger atomic charges than those in the corresponding Al_3P_3 form (a11). In b7, there is almost a factor of 2 difference in the atomic charges within the cluster. Both S_2 and S_3 have atomic charge of $-0.83e$, but S_1 has a charge of $-1.65e$. The difference in charges between Mg_2 (and Mg_3) ($+0.87e$) and Mg_1 ($+1.58e$) is large. This difference in ionic character makes the Mg_1–S_1 bond length shorter than the other Mg–S bond lengths. A similar, but less pronounced effect was observed in a11 above.

Besides the three structures b5, b6, and b7, we optimized other structures similar to the ones studied in the AIP case. However, they did not lead to any other local minima. Some of the structures such as those analogous to a5 and a9 collapsed to the planar form after considerable rearrangement. All others either collapsed to one of the three minima or yielded high energy forms such as dissociated Mg_2S_3 plus a Mg atom. Among all the starting structures we considered for Mg_3S_3, the above three structures are the lowest energy forms.

As shown in Table II, the planar D_{3h} symmetry structure is the lowest energy structure for the Mg_3S_3 cluster. At the MP4/6-31G* level, b5 is 75 kcal/mol lower in energy than b7 and 137 kcal/mol lower in energy than b6. The order of stability of the three structures is unchanged on going from the MP4/6-31G* level to the more sophisticated calculations with the QCISD(T) and the larger basis set corrections. The relative energies of b7 and b6 are slightly lowered to become 68 and 125 kcal/mol higher than b5 at these higher levels of theory. Thus there is one clearcut planar ground state structure for Mg_3S_3. This is in contrast to Al_3P_3, where the three-dimensional structure (Si_6-like structure) is the most stable structure. The difference is clearly attributable to the importance of ionic bonding contributions in Mg_3S_3.

BONDING ANALYSIS

In this section, we compare the nature of the hybridization and bonding in the mixed clusters considered in this study. We focus particular attention on the dimers Al_2P_2 and Mg_2S_2, since the trimers show the same effects in a slightly more complicated manner.

First we consider the ground state isomer of Al_2P_2 (a2). In the current discussion, the molecule is oriented in the yz plane with the y axis along the short diagonal. As mentioned earlier, the charge on the atoms is $\pm 0.61e$. After neglecting the small $3d$ population, the hybridization on the Al (Table V) is $3s^{1.87}\,3p^{0.50}$, showing clearly that the charge flow is principally from the $3p$ orbitals on Al to P. In particular, the charge flow is along the σ bonds with the maximum gain on the P atoms being on the p_z orbitals which have the highest components pointing towards the Al atoms. There are two π electrons with almost all the corresponding p_x populations being on the phosphorus atoms. Thus the π bond is principally between the two P atoms. Thus, a2 can be considered as double bonded (P = P) which is bridged by two Al atoms. Electrostatic effects keep Al apart, thus forming a planar rhombus. The P–P distance in a2 (2.04 Å) is clearly consistent with the presence of a double bond (P–P single bond distance is typically 2.20 Å).[44]

This bonding picture of a2 is in contrast to the isoelectronic Si_4 cluster where the Si–Si bond along the short diagonal is weak and the π bond is along the perimeter of the ring.[12] Nevertheless, the orbital configurations between Si_4 and a2 do correlate, making it possible to classify a2 as a "Si_4-like" cluster.

The other structure a3 is clearly quite different. First, the charges on the atoms are much larger ($\pm 1.10e$), thus the electrostatic factors play a much larger factor as discussed earlier. The hybridization on the Al atoms is $3s^{0.87}3p^{0.96}$, as shown in Table V. This is clearly counterintuitive since all the charge which is lost comes from the $3s$ orbital (relative to the s^2p^1 atom) which is expected to be significantly lower in energy. A more consistent picture of the bonding in a3 can be derived by considering it as resulting from the interaction of promoted (s^1p^2) Al atoms with P atoms. The resulting stronger interaction partially offsets the promotion energy required, though it is clearly insufficient to make a3 more stable. The charge flow from Al to P is now both along the σ bond (mostly p_z) and the π bond (p_x). Thus, if we interact two Al atoms ($s^1p_x^1p_z^1$) with two P atoms ($s^2p_x^1p_y^1p_z^1$), the resulting electronic configuration would be consistent with that of a3. The principal difference from a2 is that a3 has four π electrons (two π electrons in a2). The p_x population of $0.34e$ on Al and $1.64e$ on P indicates that there is a π-electron transfer of about $0.6e$ from Al to P. The σ-electron transfer of about $0.5e$ is comparable to that of a2. Thus the overall charges are much larger. The Al–P distance in a3 (2.27 Å) is consistent with this picture, being considerably shorter than that in a2 (2.53 Å). Nevertheless, the necessary electron promotion and the lack of P–P bonding makes a3 34 kcal/mol less stable than a2.

The bonding in Mg_2S_2 is simpler to interpret. Since the Mg atom has a $3s^2$ electronic configuration, promotion to $3p$

orbitals is necessary in order to form a covalent bond. The only structure with significant Mg p-orbital population is b6 which is the analog of Si_6. All other forms have only very small $3p$ populations.

First we consider the ground state structure b2 where the charges are large $\pm 1.54e$. It has four π electrons that result from the interaction of a Mg atom (s^2) with a S atom ($s^2p_x^2p_y^1p_z^1$). The electron transfer is in the plane of the molecule, efficiently utilizing the overlap between the s orbital on Mg and the p_y, p_z orbitals on S.

The other structure b3 is somewhat different. It has only two π electrons that result from the interaction of Mg atoms (s^2) with S atoms ($s^2p_x^1p_y^2p_z^1$). The electron transfer is now efficient for only one electron (into the p_z orbital on S). Since the $3s$ orbitals on Mg do not overlap with the p_x (π orbitals) of S, electron transfer into the p_x orbitals in the D_{2h} structure is not directly possible. Thus, the charge on Mg is only about $+0.9e$ in this form, making it less stable than b2. However, it may be noted that a puckering distortion away from D_{2h} symmetry may allow a more efficient electron transfer due to the admixture of the σ and π orbitals in the C_{2v} form. However, too much puckering is unlikely since it would result in increasing the electrostatic repulsion between the Mg atoms. At the HF/6-31G* level, the puckering away from D_{2h} symmetry is significant. However, reoptimization at the MP2/6-31G* level indicates a much lower degree of puckering. The change in geometry is indicative of the competition between opposing forces in the structure.

The trimers behave similarly. Thus the hybridizations and atomic charges in the planar trimers a4 and b5 are very similar to those in the dimers a3 and b2, being more ionic than other isomers. The Si_6-like structure for Al_3P_3 (a7) is very similar to the Si_4-like form a2. The analogous Mg_3S_3 structure (b6) shows significant differences from b3, reflecting the substantial geometry change. Nevertheless, b6 shows some $3p$ populations on Mg, indicating the presence of some covalent bonding. The prismatic structure for Al_3P_3 (a11) and Mg_3S_3 (b7) appears to be intermediate between the earlier structures considered.

INTERCOMPARISONS OF DIFFERENT SIZED CLUSTERS

It was seen earlier that the calculated binding energies of the diatomic systems AlP and MgS are similar (roughly 2.1 eV). However, the nature of the ground electronic states are quite different. These binding energies are much smaller than the corresponding binding energy (3.2 eV) of the isoelectronic Si_2 cluster.[12]

In this section, we compare the binding energies of the larger clusters of MgS and AlP. The dimerization energy 2 $AlP \rightarrow Al_2P_2$ is 5.1 eV (Table I), somewhat larger than the corresponding value of 4.7 eV for 2 $MgS \rightarrow Mg_2S_2$ (Table II). As seen from the Tables I and II, the larger basis set effects are much more important for Al_2P_2, consistent with the larger contribution of covalent bonding in this system.

The trimerization energies, on the other hand, are quite similar, 9.7 eV for Al_3P_3 and 9.4 eV for Mg_3S_3. The comparative stability of Al_3P_3 is due to its three-dimensional geometry which permits the formation of more covalent bonds. The planar structure of Mg_3S_3 has relatively fewer interactions.

We can speculate on the possible structures of larger clusters. The obvious candidate for the ground state structure of Mg_4S_4 is a three-dimensional cubic form (or more correctly a T_d structure with two interpenetrating tetrahedra) which maximizes electrostatic interactions. The presence of three-dimensional charge alternation clearly would enhance its stability considerably. An analogous structure is also possible for Al_4P_4, though capped octahedral structures similar to Si_8 are also likely to be important.

CONCLUSION

Our results indicate that the difference in electronegativity is a very important factor in determining the structures of small clusters. Ionic factors are clearly dominant for MgS clusters. Thus, both Mg_2S_2 and Mg_3S_3 have planar ground state geometries where charge alternation is utilized effectively. AlP clusters, on the other hand, behave intermediate between the ionic MgS clusters and the covalent Si clusters. Thus, while the ground state structures of Al_2P_2 and Al_3P_3 are analogous to Si_4 and Si_6, other low-lying minima analogous to Mg_2S_2 and Mg_3S_3 are also found. The hybridization and bonding in the different structures are discussed in detail.

[1] E. A. Rohlfing, D. M. Cox, and A. Kaldor, J. Phys. Chem. **81**, 3322 (1984).
[2] H. W. Kroto, J. R. Heath, S. C. O'Brien, R. F. Curl, and R. E. Smalley, Nature **318**, 162 (1985).
[3] W. Krätschmer, L. D. Lamb, K. Fostiropoulos, and D. R. Huffman, Nature **347**, 354 (1990).
[4] K. Raghavachari and J. S. Binkley, J. Chem. Phys. **87**, 2191 (1987).
[5] W. L. Brown, R. R. Freeman, K. Raghavachari, and M. Schlüter, Science **235**, 860 (1987).
[6] L. A. Bloomfield, R. R. Freeman, and W. L. Brown, Phys. Rev. Lett. **54**, 2246 (1985).
[7] J. R. Heath, Y. Liu, S. C. O'Brien, Q.-L. Zhang, R. F. Curl, F. K. Tittel, and R. E. Smalley, J. Chem. Phys. **83**, 5520 (1985).
[8] M. F. Jarrold and J. E. Bower, J. Phys. Chem. **92**, 5702 (1988); **86**, 4245 (1987).
[9] M. L. Mandich, W. D. Reents, and V. E. Bondybey, J. Phys. Chem. **90**, 2315 (1986); M. L. Mandich, V. E. Bondybey, and W. D. Reents, J. Chem. Phys. **86**, 4245 (1987).
[10] K. Balasubramanian, Chem. Phys. Lett. **125**, 400 (1986); **135**, 283 (1987).
[11] P. Ballone, W. Andreoni, R. Car, and M. Parrinello, Phys. Rev. Lett. **60**, 271 (1988); W. Andreoni and G. Pastore, Phys. Rev. B **41**, 10 243 (1990).
[12] K. Raghavachari and V. Logovinsky, Phys. Rev. Lett. **55**, 2853 (1985); K. Raghavachari, J. Chem. Phys. **84**, 5672 (1986); K. Raghavachari and C. M. Rohlfing, Chem. Phys. Lett. **143**, 428 (1988); J. Chem. Phys. **89**, 2219 (1988).
[13] U. Röthlisberger and W. Andreoni, J. Chem. Phys. **94**, 8129 (1991).
[14] C. Brechignac, P. Cahuzac, and J. P. Roux, Chem. Phys. Lett. **127**, 445 (1986).
[15] K. Balasubramanian and P. Y. Feng, J. Chem. Phys. **94**, 6664 (1991); S. Katicioğlu and S. Erkoc, J. Cryst. Growth **96**, 807 (1989); U. Meier, S. D. Peyerimhoff, and F. Grein, Z. Phys. D **17**, 209 (1990).
[16] R. O. Jones and D. Hohl, J. Chem. Phys. **92**, 6710 (1990).
[17] K. Raghavachari, R. C. Haddon, and J. S. Binkley, Chem. Phys. Lett. **122**, 219 (1985).
[18] R. Stendel, Topics Current Chem. **102**, 149 (1982).
[19] D. Hohl, R. O. Jones, R. Car, and M. Parrinello, J. Chem. Phys. **89**, 6823 (1988).
[20] K. Raghavachari, C. M. Rohlfing, and J. S. Binkley, J. Chem. Phys. **93**, 5862 (1990).

[21] S. C. O'Brien, Y. Liu, Q. L. Zhang, J. R. Heath, F. K. Tittle, R. F. Curl, and R. E. Smalley, J. Chem. Phys. **84**, 4074 (1986).
[22] G. W. Lemire, G. A. Bishea, S. A. Heidecke, and M. D. Morse, J. Chem. Phys. **92**, 121 (1990); K. Balasubramanian, J. Mol. Spectrosc. **139**, 405 (1990).
[23] C. Jin, K. J. Taylor, J. Conceicao, and R. E. Smalley, Chem. Phys. Lett. **175**, 17 (1990).
[24] L. Lou, L. Wang, L. P. F. Chibante, R. T. Laaksonen, P. Nordlander, and R. E. Smalley, J. Chem. Phys. **94**, 8015 (1991).
[25] U. Meier, S. D. Peyerimhoff, and F. Grien, Chem. Phys. **150**, 331 (1991); K. Balasubramanian, Chem. Phys. Lett. **177**, 58 (1990).
[26] K. D. Kolenbrander and M. Mandich, J. Chem. Phys. **92**, 4759 (1990).
[27] L. Brus, J. Phys. Chem. **90**, 2555 (1986); M. G. Bawendi, M. L. Steigerwald, and L. E. Brus, Annu. Rev. Phys. Chem. **41**, 477 (1990).
[28] N. G. Phillips, C. W. S. Conover, and L. A. Bloomfield, J. Chem. Phys. **94**, 4980 (1990).
[29] M. A. Al-Laham and K. Raghavachari, Chem. Phys. Lett. (in press).
[30] For a general introduction to Hartree–Fock-based methods, see W. J. Hehre, L. Radom, P. v. R. Schleyer, and J. A. Pople, *Ab Initio Molecular Orbital Theory* (Wiley, New York, 1986).
[31] W. J. Hehre, R. Ditchfield, R. F. Stewart, and J. A. Pople, J. Chem. Phys. **52**, 2769 (1970).
[32] M. S. Gordon, J. S. Binkley, J. A. Pople, W. J. Pietro, and W. J. Hehre, J. Am. Chem. Soc. **104**, 2797 (1982).
[33] M. M. Francl, W. J. Pietro, W. J. Hehre, J. S. Binkley, M. S. Gordon, D. J. DeFrees, and J. A. Pople, J. Chem. Phys. **77**, 3654 (1982).
[34] J. A. Pople, R. Krishnan, H. B. Schlegel, and J. S. Binkley, Int. J. Quantum Chem. Symp. **13**, 255 (1979).
[35] J. A. Pople, H. B. Schlegel, R. Krishnan, D. J. DeFrees, J. S. Binkley, M. J. Frisch, R. A. Whiteside, R. F. Hout, and W. J. Hehre, Int. J. Quantum Chem. Symp. **15**, 269 (1981).
[36] R. Krishnan, M. J. Frisch, and J. A. Pople, J. Chem. Phys. **72**, 4244 (1980), and references cited therein.
[37] J. A. Pople, M. Head-Grodon, and K. Raghavachari, J. Chem. Phys. **87**, 5968 (1987).
[38] K. Raghavachari, G. W. Trucks, J. A. Pople, and E. Replogle, Chem. Phys. Lett. **158**, 207 (1989).
[39] A. D. McLean and G. S. Chandler, J. Chem. Phys. **72**, 5639 (1980).
[40] The 2*d* exponents used are 0.9 and 0.225; the *f* exponent is 0.32.
[41] J. P. Foster and F. Weinhold, J. Am. Chem. Soc. **102**, 7211 (1980).
[42] A. E. Reed, R. B. Weinstock, and F. Weinhold, J. Chem. Phys. **84**, 2428 (1986).
[43] E. Kaufmann, K. Raghavachari, A. E. Reed, and P. v. R. Schleyer, Organometallics **7**, 1597 (1988).
[44] *CRC Handbook of Chemistry and Physics*, 65th ed., edited by R. C. Weast (CRC, Boca Raton, Fla., 1985).
[45] U. Meier, S. D. Peyerimhoff, P. S. Bruna, S. P. Karna, and F. Grien, Chem. Phys. **130**, 311 (1989).
[46] K. P. Huber and G. Herzberg, *Molecular Spectra and Molecular Structure* (Van Nostrand–Reinhold, New York, 1979), Vol. 4.
[47] The Mg–S bulk bond length is estimated to be the average of Mg–Mg and S–S bulk bonds.